

Article

The Systematic Adsorption of Diclofenac onto Waste Red Bricks Functionalized with Iron Oxides

Ziyang Zhang ¹, Yuxiu Li ², Hongrui Chen ³, Xiaoran Zhang ¹ and Haiyan Li ^{1,*}

¹ Beijing Engineering Research Center of Sustainable Urban Sewage System Construction and Risk Control, Beijing University of Civil Engineering and Architecture, Beijing 100044, China; ziyangzhang@126.com (Z.Z.); zhangxiaoran@bucea.edu.cn (X.Z.)

² Beijing Urban Green Source Environmental Protection Technology Cooperation, Beijing 102601, China; lyx01016427@163.com

³ CRRC Environmental Science & Technology Cooperation, Beijing 100067, China; hr630@126.com

* Correspondence: lihaiyan@bucea.edu.cn; Tel.: +86-10-6832-2452

Received: 17 August 2018; Accepted: 24 September 2018; Published: 28 September 2018



Abstract: In this study, waste red bricks were incorporated with iron oxides (goethite and hematite) and used for the removal of diclofenac (DCF) from aqueous solutions. The prepared waste red bricks were systematically characterized by XRF, XRD, BET, and SEM. The batch experiments were systematically conducted by investigating the adsorption kinetics, isotherms, thermodynamics, pH, and ionic strength effect. Results showed that the incorporation of iron oxides could enhance the adsorption capacity of DCF onto waste bricks, while the increased effect of hematite was better than goethite. DCF was adsorbed rapidly onto waste bricks, and the adsorption kinetic fitted the pseudo-second-order model perfectly, which could be attributed to the strong interaction between DCF and iron oxides. The increasing pH values decreased the adsorption capacity greatly, which may be due to the electrostatic repulsive interactions. The adsorption of DCF onto waste bricks was an exothermic reaction, and the adsorption isotherms fitted well with the Langmuir model. This study offers new guidelines for the utilization of construction waste, and shows useful methods for the elimination of micropollutants from aqueous solution.

Keywords: waste bricks; goethite; hematite; adsorption; diclofenac

1. Introduction

In the last few decades, great concern has been raised on the increasing number of emerging compounds which were detected at different levels in diverse water environments, such as wastewater, surface water, groundwater, and even drinking water [1,2]. These compounds contain a lot of natural or synthetic chemicals, such as pharmaceuticals and personal care products, endocrine disrupting compounds, persistent organic pollutants, and pesticides [3]. However, results showed that the conventional water treatment had little effect on the elimination of these materials, due to their ubiquitous and non-biodegradable characteristics [4].

As one of the most typical pharmaceuticals and personal care products, diclofenac (DCF) is a widely prescribed non-steroidal anti-inflammatory drug. Due to the large amount of usage (940 tons per year), DCF could enter into the environment through different pathways, such as direct disposal, hospital effluents, and wastewater treatment plant discharges [5,6]. Although the concentration of DCF in environments is low, results show that it has adverse effects on aquatic life and humans [7–9]. Therefore, it has become urgent to find new useful methods for the removal of DCF from aqueous solutions.

In recent years, many studies have been conducted for the elimination of DCF from wastewater by either batch or column experiments [10–14]. Among these methods, adsorption remains attractive

because of its advantages, such as simplicity, reliability, and cost effectiveness. Many adsorbents have been investigated for the removal of DCF from aqueous solutions, such as activated carbon, zeolite, chitosan, and graphene oxide [5,15,16]. Although these materials showed extremely high adsorption of DCF, the materials' cost is also high, which restricts the application. As the key factor of the adsorption process, adsorbents should gain more attention as they would be low cost, have high adsorption capacity, and be environmental friendly.

As a developing country, urbanization has developed rapidly recently in China, and the amount of construction waste increased sharply. As one of the more common examples of construction waste, waste bricks could cause various environmental problems. The investigation of utilizing waste bricks as adsorbents has drawn great attention, due their proper surface area, micropore volume, and porous structure [17,18]. Although recent studies have demonstrated that waste bricks can be used as a low-cost adsorbent for the removal of pollutants, compared with commercial adsorbents, the lower adsorption capacity inhibits their application in water treatment. Iron oxides have shown considerable promise for the removal of contaminants due to their ubiquitous properties, especially for micropollutants [19]. For example, as the typical iron oxides, goethite and hematite were demonstrated to be useful adsorbents for the removal pollutants from aqueous solutions [15,20]. However, most of such pure iron oxides have relatively low surface area, and the numbers of useful active sites are limited, which inhibits the use of these iron oxides in water treatment. Results also show that the impregnation of iron oxides onto conventional adsorbents could enhance the adsorption capacity and promote the utilization of iron oxides [11,15].

In this study, without dramatically modifying the original structure of the waste bricks, two typical iron oxides (goethite and hematite) were selected for the functionalization of waste red bricks, and the prepared adsorbents were used for the removal of DCF from aqueous solutions. The prepared waste bricks were characterized systematically by XRF (X-Ray Fluorescence), XRD (X-ray diffraction), BET (Brunner–Emmet–Teller), and SEM (Scanning Electron Microscope). The adsorption process of DCF onto prepared adsorbents was carried out by batch experiments and the factors affecting the adsorption, such as kinetics, pH, thermodynamics, and ionic strength, were investigated. This study could offer new guidelines for the utilization of construction waste and show useful methods for the elimination of micropollutants from aqueous solution.

2. Materials and Methods

2.1. Materials and Chemicals

The diclofenac sodium salt (>99%) was purchased from Sigma Aldrich Chemical Co. (Madison, WI, USA), and used without further purification. The stock solution of DCF was prepared at 1 g/L, and was diluted to the desired concentrations before the experiments. The chemical formula of diclofenac sodium is $C_{14}H_{10}Cl_2NNaO_2$, and the molecular weight is 318.14. The protonation constant (pK_a) of DCF is 4.15. Methanol and acetonitrile were HPLC (High Preussner Liquid Chromatography) grade and obtained from Fisher Scientific Corp. All other chemicals, such as hydrochloric acid, nitric acid, $FeSO_4 \cdot 7H_2O$, $NaHCO_3$, $Fe(NO_3)_3 \cdot 9H_2O$, NaCl, KOH, and NaOH were all of analytical grade. Ultrapure water (MilliQ) was used in all experiments.

2.2. The Preparation of Adsorbents

In this study, three different kinds of waste red bricks were prepared: pickling red brick particles (PRBP), goethite-coated brick particles (GCBP), and hematite-coated brick particles (HCBP). The method of preparation of GCBP and HCBP was carried out according to Schwertmann [21].

PRBP: The waste red bricks were firstly collected at Beijing University of Civil Engineering and Architecture. Then, the bricks were broken into grain and sieved to the size of 0.5 to 1.0 mm. The obtained particles were then soaked in acid solution (HCl 6 mol/L) at 90 ± 1 °C for 24 h. The slurry

was filtered through 0.45 microns polytetrafluoroethylene membrane filter and washed with ultrapure water several times, dried at 105 ± 1 °C, and the final PRBP was obtained.

GCBP: First, 0.05 mol/L FeSO_4 solution were prepared by adding $\text{FeSO}_4 \cdot 7\text{H}_2\text{O}$ into ultrapure water after N_2 was bubbled through for 30 min. Second, 1 mol/L NaHCO_3 solution was added into the solution where the N_2 was replaced by air. Third, a certain amount of PRBP was added into the solution, and the slurry was stirred continuously for 48 h. The solution pH values were maintained at 7.0 ± 0.1 by NaHCO_3 buffer solution. Oxidation was completed when the color of the suspension changed from green-blue to ochreous. The resultant product was then filtered by a 0.45 microns polytetrafluoroethylene membrane filter, and washed thoroughly until a clear supernatant was obtained. The GCBP was finally obtained by freeze-drying.

HCBP: First, 0.2 mol/L $\text{Fe}(\text{NO}_3)_3$ solution was prepared by adding certain $\text{Fe}(\text{NO}_3)_3 \cdot 9\text{H}_2\text{O}$ into preheated ultrapure water. Second, 1 mol/L KOH and 1 mol/L NaHCO_3 solutions were added into the mixture. Third, a certain amount of PRBP was added into the solution and the mixture was held in a closed polyethylene flask at 90 °C for 48 h. The resultant product was cooled to room temperature, filtered, and washed thoroughly with ultrapure water until a clear supernatant was obtained. The HCBP was finally obtained also by freeze-drying.

2.3. Characterization Techniques

The surface morphology of waste red bricks was examined by scanning electron microscopy (SEM, Limited S-4800, Hitachi, Tokyo, Japan). The X-ray powder diffraction (XRD) patterns of bricks were obtained by an X-ray diffractometer (XRD, D8 ADVANCE, Bruker, Germany) with $\text{Cu K}\alpha$ radiation. The chemical analysis of waste red bricks was carried out using an X-ray fluorescence spectrometer (XRF, XRF-1800, Shimadzu, Tokyo, Japan). N_2 adsorption isotherms were collected at 77 K on a Micromeritics (ASAP 2020 HD88, Mike, Atlanta, GA, USA), and the pore volume and pore size distribution were calculated using a BJH (Barret–Joyner–Halenda) method. The bricks were digested with acid mixture using a constant temperature electric heating plate, and Fe (III) contents was determined by atomic absorption spectrophotometry (Z-2010, Hitachi, Tokyo, Japan).

2.4. Adsorption Experiments

The batch experiment was conducted to investigate the adsorption behavior of DCF onto PRBP, GCBP, and HCBP. All batch experiments were conducted in the dark to inhibit the potential photodegradation. In this study, all the tests were performed in duplicate, and the values listed in the figures were calculated by the average.

In the kinetics experiments, three sets of 500 mL solutions were prepared with the DCF concentration of 5 mg/L. The PRBP, GCBP, and HCBP were then added into the solution with a dosage of 2 g/L. The mixed solution was stirred continuously with a speed of 170 rpm, and the solution pH values were maintained at 7.0 ± 0.1 by 0.1 mol/L HCl or NaOH solutions. The samples were taken at appropriate time intervals, filtered through a 0.22 μm polytetrafluoroethylene membrane filter, and the concentration of DCF in the solution was analyzed.

Adsorption isotherms and thermodynamics experiments were conducted by adding 0.06 g PRBP, GCBP, and HCBP into 30 mL solutions with the DCF concentration of 1–40 mg/L. The solution pH values were maintained at 7.0 ± 0.1 , and the temperature was maintained at 298, 308, and 318 K. The mixed solution was stirred continuously with a speed of 170 rpm for 24 h to reach equilibrium. Other experimental conditions were the same as in the kinetics experiments.

The effect of pH values and ionic strength were conducted by adding 0.06 g PRBP, GCBP, and HCBP into 30 mL solutions with the DCF concentration of 5 mg/L. The solution pH was adjusted and maintained to desired values in the range of 4.0–9.0. The ionic strength effect was studied with different ionic strength (0.001–0.2 mol/L NaCl), and the solution pH was maintained at 7.0 ± 0.1 . Other experimental conditions were the same as in the kinetics experiments.

The concentrations of DCF were determined by Ultra Performance Liquid Chromatography (UPLC, Acquity, Waters, CA, USA) at a wavelength of 265 nm, using a C₁₈ reverse-phase column (100 mm × 2.1 mm and 1.7 μm particle size). The mobile phase consisted of 20% ultrapure water (0.01% CH₃COOH) and 80% methanol at a flow rate of 0.4 mL/min.

3. Results and Discussion

3.1. The Characteristics of PRBP, GCBP, and HCBP

The results of XRF, BET, pore size, and Fe content are illustrated in Table 1. As shown in XRF, the waste red bricks consist of Si₂O, Al₂O₃, Fe₂O₃, and others. After functionalization with the iron species, the main composition of waste red bricks was mainly unchanged, while the amount of coated iron in GCBP and HCBP was 3.18 and 2.29 mg/g, respectively. Furthermore, although the specific surface area of GCBP and HCBP decreased from 10.42 to 6.93 and 2.43 m²/g, the average pore size increased from 4.52 to 5.35 and 5.80 nm, which may be more useful for the removal of pollutants from aqueous solutions. These results were consistent with the study of impregnated iron species onto activated carbon [22].

Table 1. The properties of pickling red brick particles (PRBP), goethite-coated brick particles (GCBP), and hematite-coated brick particles (HCBP).

Adsorbents	Element Content (%) XRF				BET (m ² /g)	Pore Size (nm)	Coated Fe (mg/g)
	Si ₂ O	Al ₂ O ₃	Fe ₂ O ₃	CaO			
PRBP	72.57	13.97	4.12	1.53	10.42	4.52	-
GCBP	73.02	13.67	4.17	1.33	6.93	5.35	3.18
HCBP	71.88	14.12	4.20	1.46	2.43	5.80	2.29

The N₂ adsorption/desorption curves and corresponding BJH pore size distribution of PRBP, GCBP, and HCBP were presented in Figure 1. According to the IUPAC (International Union of Pure and Applied Chemistry) classification, it has been observed that all three N₂ adsorption/desorption curves belonged to type IV isotherms with hysteresis loops between adsorption and desorption branches, indicated the presence of a porous structure on the adsorbent [1]. Besides, compared with PRBP, the higher P/P₀ and hysteresis of GCBP verified the larger pore size, which was shown in Table 1. All these results showed that the main structure of waste red bricks was maintained after the incorporation of iron species.

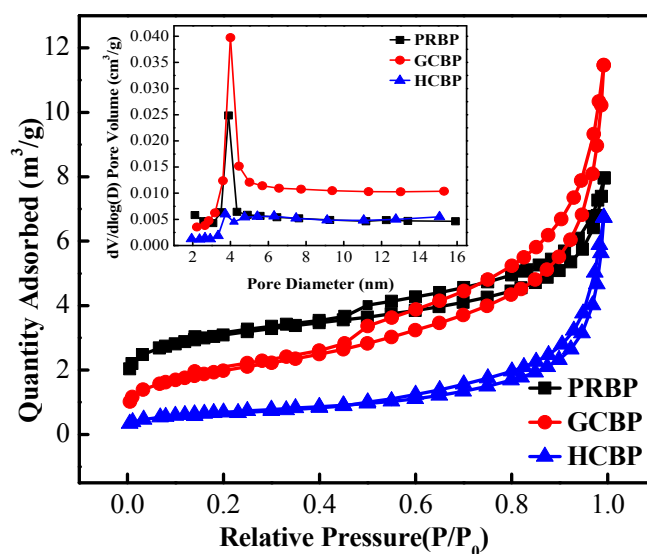


Figure 1. N₂ adsorption/desorption isotherms and corresponding BJH pore size distribution.

The XRD patterns of PRBP, GCBP, and HCBP are shown in Figure 2. After functionalization with hematite and goethite, compared with the results of PRBP, the main diffraction patterns of bricks were almost identical, which suggested the main structure and composition of waste red bricks were nearly unchanged. However, the XRD patterns of GCBP show several new well-defined characteristic peaks of (110), (120), (111), (121), and (151), suggesting the presence of goethite structure on the adsorbent, which indicated that goethite was successfully incorporated into the red bricks [23]. In the same way, the new peaks of (012), (110), and (024) in the patterns of HCBP indicated the successful incorporation of hematite onto waste red bricks [19]. These results were associated with the increasing quantity of deposited iron oxide in Table 1.

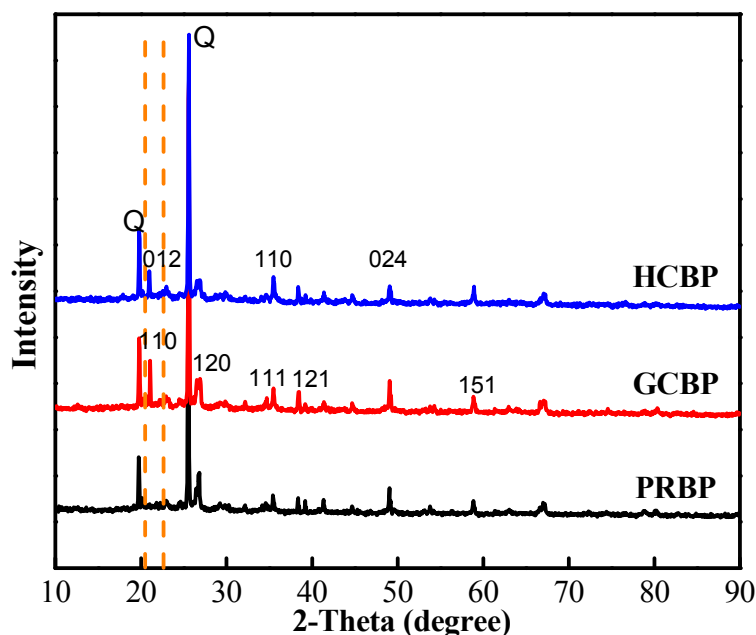


Figure 2. The X-ray diffraction patterns of PRBP, GCBP, and HCBP.

Representative SEM images of PRBP, GCBP, and HCBP are depicted in Figure 3. Figure 3a showed that the virgin red bricks had a relatively irregular and rough surface, small cracks and pores. After the incorporation of hematite and goethite, Figure 3b,c show a similar disordered structure, but unevenly distributed fine particles are observed on the surface, which may be attributed to the immobilization of goethite and hematite onto the solid surface. Furthermore, both goethite and hematite did not change the surface properties and main structure of waste red bricks.

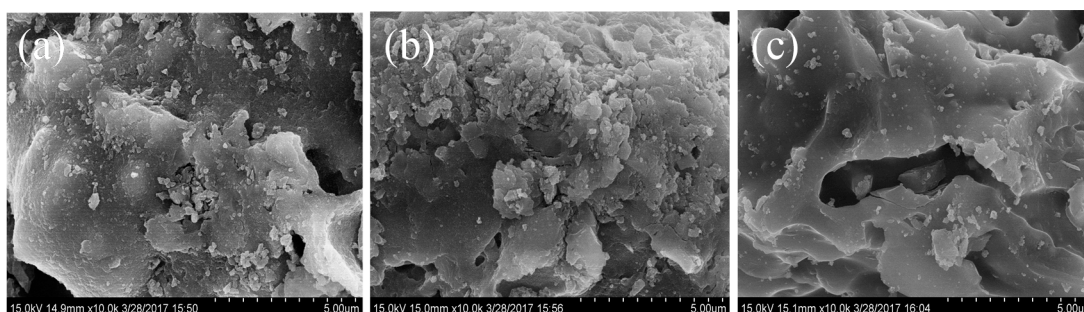


Figure 3. The SEM images of PRBP (a), GCBP (b), and HCBP (c).

3.2. The Adsorption Kinetics of DCF onto PRBP, GCBP, and HCBP

Figure 4 showed the adsorption kinetics of DCF onto PRBP, GCBP, and HCBP. For all three adsorbents, DCF was adsorbed rapidly in the first 60 min, followed by a relatively slow process, and

finally achieved equilibrium at 9 h. The high adsorption rate could be attributed to the roughness, high porosity, and surface area of the bricks, which enhanced the mass transfer of DCF in the adsorption process. Furthermore, the chemical structure of waste red bricks may offer abundant useful adsorption sites for DCF removal.

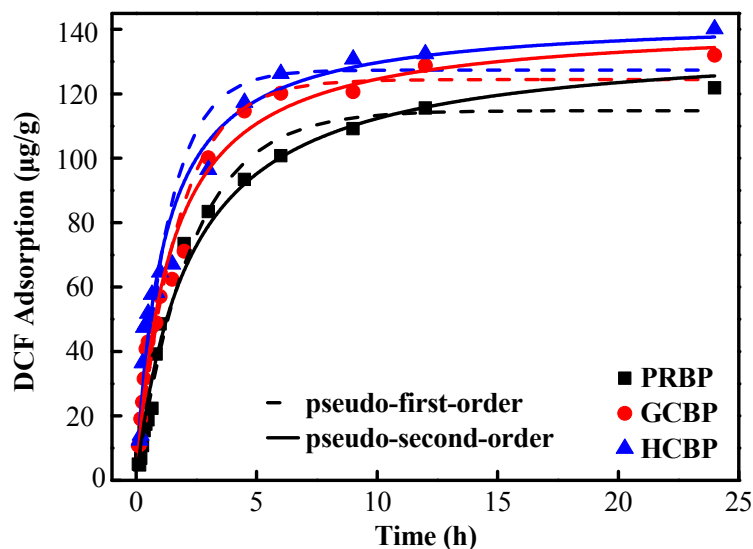


Figure 4. The adsorption kinetic of diclofenac (DCF) onto PRBP, GCBP, and HCBP. Experimental conditions: $m = 2 \text{ g/L}$, $C_0 = 5 \text{ mg/L}$, $T = 25 \pm 1 \text{ }^\circ\text{C}$, $\text{pH} = 7.0 \pm 0.1$.

To investigate the adsorption process further, the adsorption kinetics were interpreted by the pseudo-first-order and pseudo-second-order model represented by Equations (1) and (2), respectively [24].

$$\ln(Q_e - Q_t) = \ln Q_e - k_1 t \quad (1)$$

$$\frac{t}{Q_t} = \frac{1}{k_2 Q_e^2} + \frac{t}{Q_t} \quad (2)$$

where Q_e and Q_t ($\mu\text{g/g}$) are the adsorption capacity at adsorption equilibrium and time; and k_1 ($\mu\text{g/mg/h}$) and k_2 ($\mu\text{g/h}$) are the kinetic rate constants of the pseudo-first-order model and pseudo-second-order model, respectively.

The kinetic parameters and correlation coefficients were listed in Table 2. Comparing the pseudo-first and pseudo-second modes reveal that the pseudo-second-order model was more suitable for describing the adsorption of DCF onto PRBP, GCBP, and HCBP ($r^2 > 0.96$), which indicated that the adsorption of DCF onto waste red bricks may be chemisorption. Furthermore, results also showed that the K_2 and q_e followed the order of $\text{HCBP} > \text{GCBP} > \text{PRBP}$, which suggested that the incorporation of iron species enhanced the adsorption rate and capacity of DCF onto waste red bricks. These results were consistent with the adsorption of DCF onto other adsorbents, such as goethite and surfactant-modified zeolite [19,20].

Table 2. The adsorption kinetics parameters of DCF onto PRBP, GCBP, and HCBP.

Adsorbents	Pseudo-First-Order Model			Pseudo-Second-Order Model		
	K_1 ($\mu\text{g/mg/h}$)	q_e ($\mu\text{g/g}$)	r^2	K_2 ($\mu\text{g/h}$)	q_e ($\mu\text{g/g}$)	r^2
PRBP	43.6	114.8	0.988	33.1	137.2	0.988
GCBP	59.0	124.5	0.967	49.2	142.4	0.982
HCBP	75.9	127.7	0.927	63.0	144.0	0.965

3.3. Effect of pH on the Adsorption of DCF onto PRBP, GCBP, and HCBP

As illustrated in Figure 5, the solution pH values influenced the adsorption of DCF onto PRBP, GCBP, and HCBP remarkably. For all three bricks, the influence of pH values were similar, indicated that the adsorption mechanism was not changed after the functionalization of goethite and hematite. With the increase in solution pH values from 4.0 to 9.0, the adsorption capacity of DCF decreased, apparently, from 303.20, 330.50, and 345.70, to 11.03, 12.05, and 32.05 $\mu\text{g/g}$, for PRBP, GCBP, and HCBP, respectively.

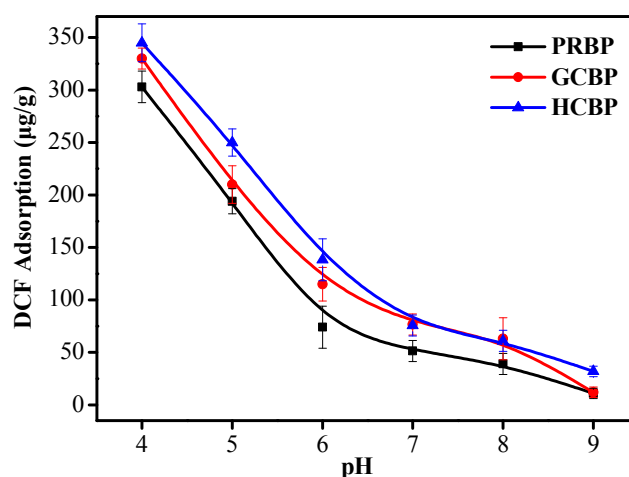


Figure 5. Effect of pH on the adsorption of DCF onto PRBP, GCBP, and HCBP. Experimental conditions: $m = 2 \text{ g/L}$, $C_0 = 5 \text{ mg/L}$, $T = 25 \pm 1 \text{ }^\circ\text{C}$.

The observed results were associated with the characteristics of DCF and surface properties of the bricks. As the pK_a value of DCF was 4.15, with the solution pH values increased from 4.0 to 9.0, and most of the DCF exhibited a negative charge. As shown in Figure 6, the charge of all bricks was mainly negative for all pH values. After the incorporation of iron oxides, the zeta potential of bricks increased, and the charge followed by the order of HCBP > GCBP, which may be attributed to the higher zero charge of hematite (8.1 vs. 6.9). With the increase in solution pH, the positive charge of adsorbents decreased, the negative charges increased, and the electrostatic repulsion between DCF and adsorbents increased, which induced the decreased adsorption capacity. Furthermore, previous reports suggested that the low solubility of DCF in acidic medium and the decrease in DCF adsorption may be attributed to the increased mobility and solubility of DCF under alkaline conditions [25].

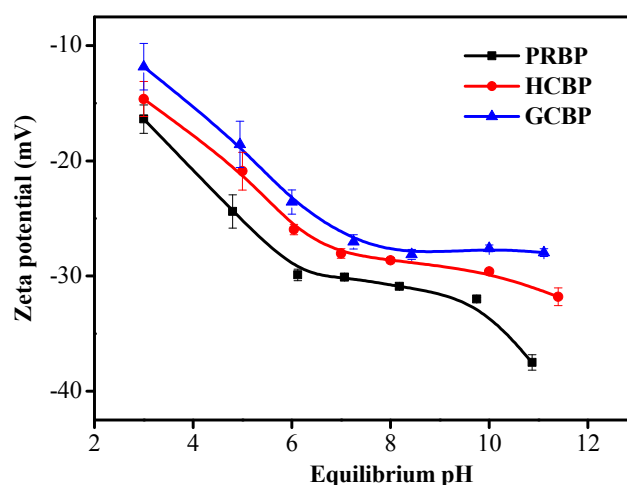


Figure 6. The zeta potential of PRBP, GCBP, and HCBP. Experimental conditions: $m = 2 \text{ g/L}$, $T = 25 \pm 1 \text{ }^\circ\text{C}$.

3.4. The Adsorption Isotherms of DCF onto PRBP, GCBP, and HCBP

Figure 7 showed the adsorption isotherm of DCF onto PRBP, GCBP, and HCBP. For all three adsorbents, the adsorption capacity of DCF increased with the increasing equilibrium concentration. Furthermore, compared with PRBP, GCBP and HCBP had a higher adsorption capacity for nearly all equilibrium concentrations, which suggested that the functionalization of iron oxide was beneficial for the removal of DCF from aqueous solution.

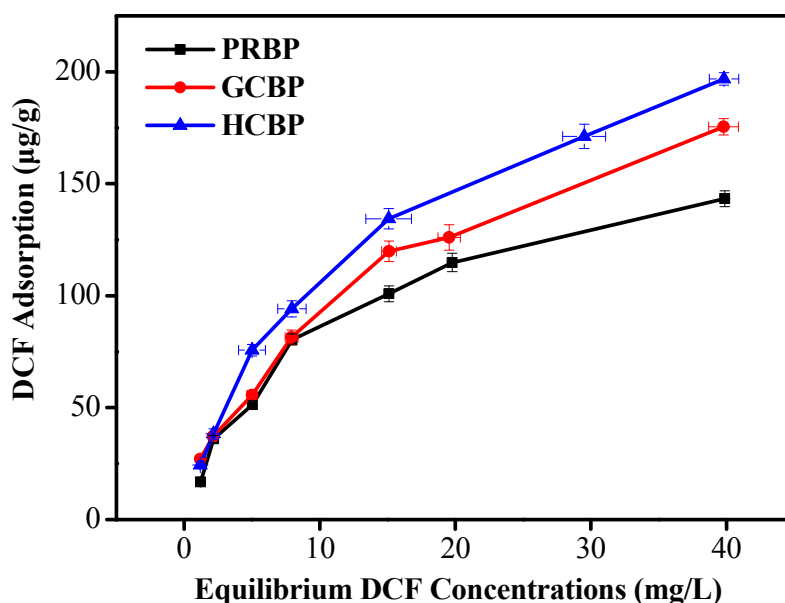


Figure 7. The adsorption isotherm of DCF onto PRBP, GCBP, and HCBP. Experimental conditions: $m = 2 \text{ g/L}$, $T = 25 \pm 1 \text{ }^\circ\text{C}$, $\text{pH} = 7.0 \pm 0.1$.

To investigate the adsorption isotherms of DCF further, the Langmuir and Freundlich isotherms were used to illustrate the adsorption behavior, and the models were presented in Equations (3) and (4), respectively. The Langmuir isotherm model is based on the assumption that each adsorption site can hold only one adsorbate molecule. The Freundlich isotherm model is commonly used to describe the adsorption characteristics for heterogeneous surface [26].

$$Q_e = \frac{Q_{max}bC_e}{1 + bC_e} \quad (3)$$

$$Q_e = K_f C_e^{\frac{1}{n}} \quad (4)$$

where C_e is equilibrium concentration (mg/L), Q_{max} is the maximum adsorption capacity of DCF onto bricks ($\mu\text{g/g}$), b is a measure of the energy of adsorption, K_f is the Freundlich adsorption constant, and n is related to the adsorption intensity.

As listed in Table 3, compared with the Freundlich model, the Langmuir model fitted the adsorption isotherms of DCF onto three bricks better ($r^2 > 0.97$), which suggested that the adsorption of DCF onto bricks was probably monolayer molecular adsorption. In addition, compared with the Q_{max} of PRBP (187.9 $\mu\text{g/g}$), the HCBP seems to be more efficient for the removal of DCF (292.3 $\mu\text{g/g}$), whereas the GCBP shows a Q_{max} of 220.5 $\mu\text{g/g}$. The adsorption capacity mainly depends on the chemical structure of red bricks and the coated iron oxides. Although the process of incorporation decreased of specific surface area of bricks (showed in Table 1), the adsorption efficiency was enhanced owing to the interaction between iron oxides and DCF. Furthermore, $1/n$ is a constant indicative of adsorption intensity or surface heterogeneity. As shown in Table 3, the values of $1/n$ for all three bricks were less than 1.0, indicating that the adsorption DCF onto bricks was favorable. These results

all indicate that waste red bricks could be used as potential adsorbents for the removal of DCF from aqueous solutions.

Table 3. The adsorption isotherm parameters of DCF.

Adsorbents	Langmuir			Freundlich		
	B (L/mg)	Q_{max} ($\mu\text{g/g}$)	r^2	K_f ($\mu\text{g/g}$)	n	r^2
PRBP	0.097	187.9	0.97	29.0	2.17	0.90
GCBP	0.078	220.5	0.98	29.8	2.06	0.97
HCBP	0.056	292.3	0.99	32.0	1.99	0.98

3.5. Effect of Ionic Strength on DCF Adsorption

To explain the adsorption mechanism of DCF onto PRBP, GCBP, and HCBP further, the influence of ionic strength on DCF adsorption were conducted, and the results were listed in Figure 8. Results showed that the increasing concentration of NaCl affected the adsorption of DCF greatly, and the influences could be divided into two regions. With the NaCl concentration increased from 0 to 0.02 mol/L, the adsorption capacity increased from 74.1, 114.9, and 138.3, to 123.8, 211.9, and 222.4 $\mu\text{g/g}$, for PRBP, GCBP, and HCBP, respectively. When the NaCl concentration increased further, the adsorption capacity of DCF decreased significantly. The enhanced adsorption of DCF onto bricks may be attributed to the charge screening effect, which can reduce the repulsion between DCF and bricks that increased the adsorption capacity greatly. However, when NaCl concentration increased further (>0.02 mol/L), abundant Cl^- in the solution could also be adsorbed onto the surface of adsorbents, and occupied part of the useful adsorption site, which decreased the adsorption capacity of DCF greatly [27]. According to the results of others, the non-specific adsorption is usually influenced greatly by the change of background electrolyte, whereas the specific adsorption is not [28]. In this study, the adsorption of DCF onto three bricks was influenced by the concentration of NaCl greatly. Thus, the adsorption of DCF onto waste red bricks could be non-specific adsorption.

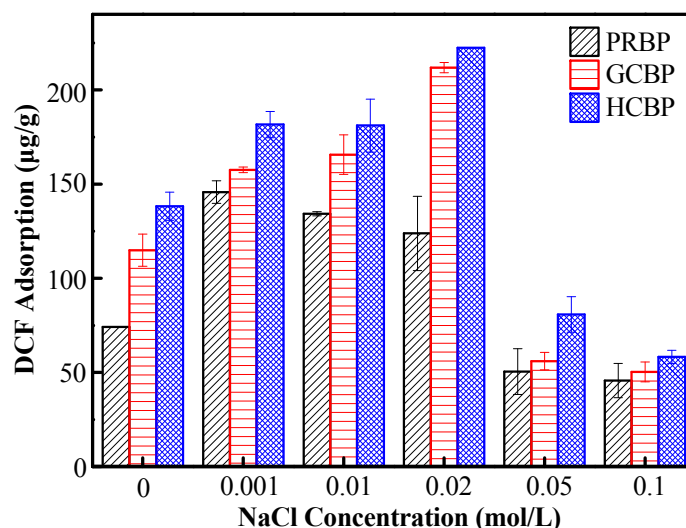


Figure 8. Effect of ionic strength on the adsorption of DCF onto PRBP, GCBP, and HCBP. Experimental conditions: $m = 2$ g/L, $C_0 = 5$ mg/L, $T = 25 \pm 1$ °C, $\text{pH} = 7.0 \pm 0.1$.

3.6. Adsorption Thermodynamics

In order to investigate the adsorption mechanism further, the temperature influences on the adsorption process were conducted at 298, 308, and 318 K, and the results were shown in Figure 9. With the temperature increase from 298 to 318 K, the adsorption capacity of DCF on all three bricks decreased, suggesting that the adsorption process was exothermic, and the adsorption was more

favorable at lower temperature. The results were consistent with other studies, which the adsorption occurred on different types of pollutants onto clay minerals and soils [26].

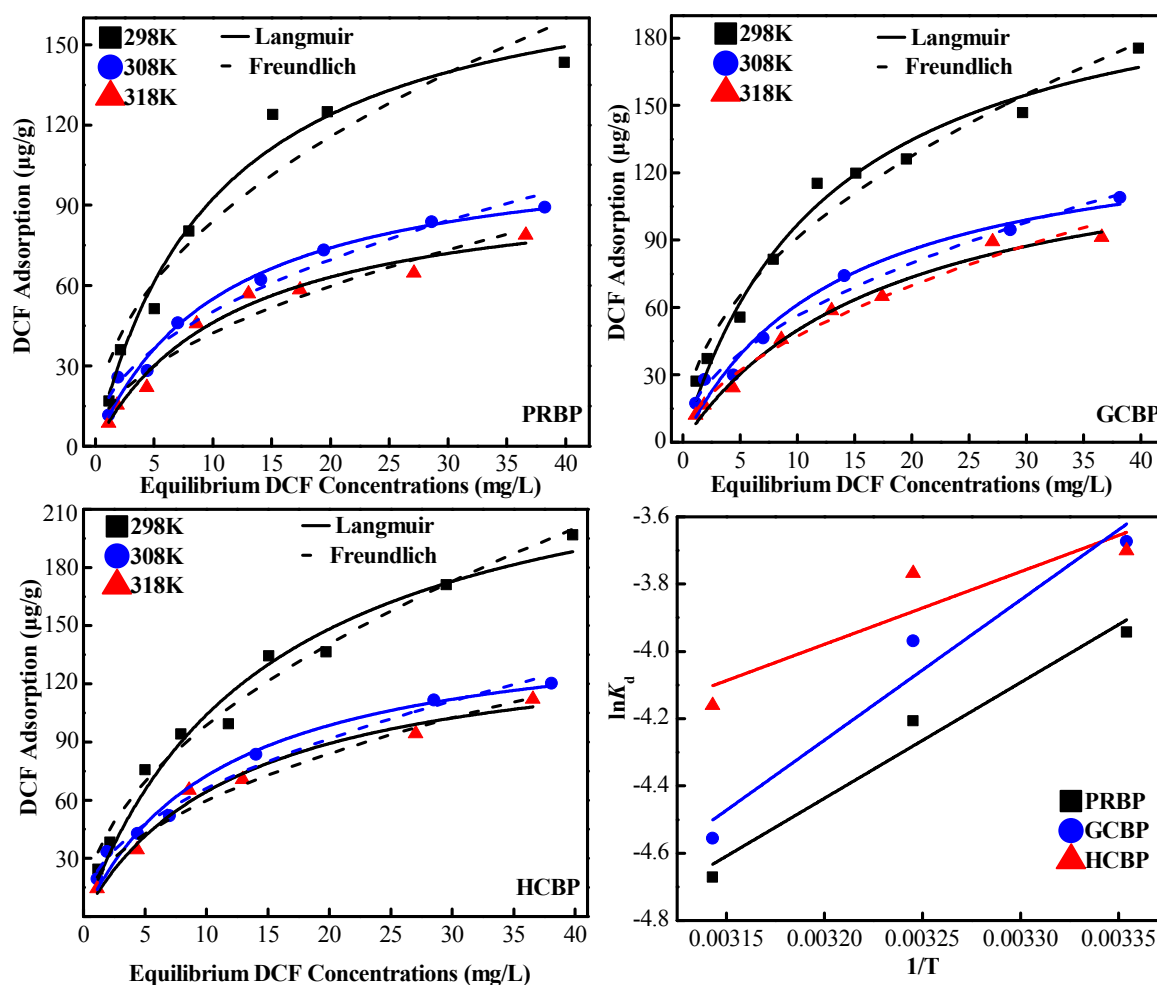


Figure 9. Effect of temperature on the adsorption of DCF onto PRBP, GCBP, and HCBP. Experimental conditions: $m = 2 \text{ g/L}$, $\text{pH} = 7.0 \pm 0.1$.

To investigate the adsorption process of DCF onto bricks further, the thermodynamic parameters were calculated by Equations (5) and (6) [29].

$$\ln K_d = \frac{-\Delta H^0}{RT} + \frac{\Delta S^0}{R} \tag{5}$$

$$\Delta G^0 = \Delta H^0 + T\Delta S^0 \tag{6}$$

where K_d is the distribution coefficient, ΔH^0 is the change of enthalpy (kJ/mol), ΔS^0 is the change of entropy (J/mol/K), ΔG^0 is the change of Gibbs free energy (kJ/mol), T is the absolute temperature in Kelvin (K), and R is the gas constant (8.314 J/mol/K).

As shown in Table 4, the negative ΔH for PRBP, GCBP, and HCBP was -28.64 , -34.70 , and -17.98 kJ/g , respectively, confirming the interaction between DCF and brick was an exothermic process. Furthermore, the negative values of ΔS were consistent with the fact that the randomness decreased during the adsorption of DCF onto waste red bricks. Simultaneously, the adsorption capacity of GCBP and HCBP was higher than PRBP at different temperatures, which suggested the functionalizations of goethite and hematite have good affinity for DCF removal.

Table 4. The thermodynamic parameters of DCF adsorption.

Adsorbents	T (K)	K_d (L/g)	ΔH (KJ/g)	ΔS (J/g/K)
PRBP	298	0.097	−28.64	−128.53
	308	0.094		
	318	0.086		
GCBP	298	0.078	−34.70	−146.49
	308	0.075		
	318	0.055		
HCBP	298	0.090	−17.98	−90.62
	308	0.089		
	318	0.080		

4. Conclusions

In this study, the adsorbents were prepared by incorporating goethite and hematite onto waste red bricks, and used for the removal of DCF from aqueous solution. Results showed that goethite and hematite were successfully incorporated onto red bricks, and the main structure of bricks was maintained. The adsorption process of DCF onto three bricks was fast and fitted the pseudo-second-order model. The adsorption isotherms fitted well with Langmuir isotherm and the Q_{max} of PRBP, GCBP, and HCBP were 187.9, 220.5, and 292.3 $\mu\text{g/g}$, which could be attributed to the strong interaction between DCF with goethite and hematite. The pH values affected the adsorption behavior greatly, and when the solution pH values increased, the adsorption capacity of DCF onto bricks apparently decreased. When the NaCl concentration increased, the adsorption capacity of DCF increased, firstly, followed by a great decrease, which suggested that the adsorption of DCF onto waste red bricks could be non-specific adsorption. Adsorption thermodynamics indicated that the adsorption process was exothermic, and the adsorption was more favorable at lower temperatures.

Author Contributions: Conceptualization and Writing-Original Draft Preparation, Z.Z.; Methodology and Investigation, Y.L. and H.C.; Data Curation and Writing-Review & Editing, X.Z. and H.L.

Funding: This research was funded by China Postdoctoral Science Foundation (2017M610039) and Natural Science Foundation of China (No. 51678025 and No. 51708014), by the Fundamental Research Funds for Beijing University of Civil Engineering and Architecture (X18132 and X18173) and Great Scholars Program (CIT&TCD20170313).

Acknowledgments: We would also like to thank Beijing Advanced Innovation Center for Future Urban Design: Sponge City Development and Water Quantity & Quality Risk Control (UDC2016040100) and Opening Projects of Beijing Advanced Innovation Center for Future Urban Design (UDC2017032922).

Conflicts of Interest: The authors declare no conflicts of interest.

References

- Xu, J.; Li, Y.; Yuan, B.; Shen, C.; Fu, M.; Cui, H.; Sun, W. Large scale preparation of Cu-doped α -FeOOH nanoflowers and their photo-Fenton-like catalytic degradation of diclofenac sodium. *Chem. Eng. J.* **2016**, *291*, 174–183. [[CrossRef](#)]
- Yang, Y.; Ok, Y.S.; Kim, K.H.; Kwon, E.E.; Tsang, Y.F. Occurrences and removal of pharmaceuticals and personal care products (PPCPs) in drinking water and water/sewage treatment plants: A review. *Sci. Total Environ.* **2017**, *596–597*, 303–320. [[CrossRef](#)] [[PubMed](#)]
- Chu, K.H.; Al-Hamadani, Y.A.J.; Park, C.M.; Lee, G.; Jang, M.; Jang, A.; Her, N.; Son, A.; Yoon, Y. Ultrasonic treatment of endocrine disrupting compounds, pharmaceuticals, and personal care products in water: A review. *Chem. Eng. J.* **2017**, *327*, 629–647. [[CrossRef](#)]
- Melvin, S.D.; Leusch, F.D.L. Removal of trace organic contaminants from domestic wastewater: A meta-analysis comparison of sewage treatment technologies. *Environ. Int.* **2016**, *92–93*, 183–188. [[CrossRef](#)] [[PubMed](#)]

5. De Oliveira, T.; Guégan, R.; Thiebault, T.; Milbeau, C.L.; Muller, F.; Teixeira, V.; Giovanela, M.; Boussafir, M. Adsorption of diclofenac onto organoclays: Effects of surfactant and environmental (pH and temperature) conditions. *J. Hazard. Mater.* **2017**, *323 Pt A*, 558–566. [[CrossRef](#)]
6. Zhang, Y.; Geißen, S.U.; Gal, C. Carbamazepine and diclofenac: Removal in wastewater treatment plants and occurrence in water bodies. *Chemosphere* **2008**, *73*, 1151–1161. [[CrossRef](#)] [[PubMed](#)]
7. Jones, O.A.; Lester, J.N.; Voulvoulis, N. Pharmaceuticals: A threat to drinking water? *Trend Biotechnol.* **2005**, *23*, 163–167. [[CrossRef](#)] [[PubMed](#)]
8. Hajj-Mohamad, M.; Darwano, H.; Duy, S.V.; Sauve, S.; Prevost, M.; Arp, H.P.; Dorner, S. The distribution dynamics and desorption behaviour of mobile pharmaceuticals and caffeine to combined sewer sediments. *Water Res.* **2017**, *108*, 57–67. [[CrossRef](#)] [[PubMed](#)]
9. Balbi, T.; Montagna, M.; Fabbri, R.; Carbone, C.; Franzellitti, S.; Fabbri, E.; Canesi, L. Diclofenac affects early embryo development in the marine bivalve *Mytilus galloprovincialis*. *Sci. Total Environ.* **2018**, *642*, 601–609. [[CrossRef](#)] [[PubMed](#)]
10. Thelusmond, J.R.; Kawka, E.; Strathmann, T.J.; Cupples, A.M. Diclofenac, carbamazepine and triclocarban biodegradation in agricultural soils and the microorganisms and metabolic pathways affected. *Sci. Total Environ.* **2018**, *640*, 1393–1410. [[CrossRef](#)] [[PubMed](#)]
11. Su, Y.M.; Jassby, D.; Song, S.K.; Zhou, X.F.; Zhao, H.Y.; Filip, J.; Petala, E.; Zhang, Y.L. Enhanced Oxidative and Adsorptive Removal of Diclofenac in Heterogeneous Fenton-like Reaction with Sulfide Modified Nanoscale Zerovalent Iron. *Environ. Sci. Technol.* **2018**, *52*, 6466–6475. [[CrossRef](#)] [[PubMed](#)]
12. Chen, W.R.; Li, X.K.; Tang, Y.M.; Zhou, J.L.; Wu, D.; Wu, Y.; Li, L.S. Mechanism insight of pollutant degradation and bromate inhibition by Fe-Cu-MCM-41 catalyzed ozonation. *J. Hazard. Mater.* **2018**, *346*, 226–233. [[CrossRef](#)] [[PubMed](#)]
13. Zambianchi, M.; Durso, M.; Liscio, A.; Treossi, E.; Bettini, C.; Capobianco, M.L.; Aluigi, A.; Kovtun, A.; Ruani, G.; Corticelli, F.; et al. Graphene oxide doped polysulfone membrane adsorbers for the removal of organic contaminants from water. *Chem. Eng. J.* **2017**, *326*, 130–140. [[CrossRef](#)]
14. Nguyen, L.N.; Hai, F.L.; Price, W.E.; Leusch, F.D.L.; Roddick, F.; McAdam, E.J.; Magram, S.F.; Nghiem, L.D. Continuous biotransformation of bisphenol A and diclofenac by laccase in an enzymatic membrane reactor. *Int. Biodeterior. Biodegrad.* **2014**, *95*, 25–32. [[CrossRef](#)]
15. Zhao, Y.; Liu, F.; Qin, X. Adsorption of diclofenac onto goethite: Adsorption kinetics and effects of pH. *Chemosphere* **2017**, *180*, 373–378. [[CrossRef](#)] [[PubMed](#)]
16. Nam, S.W.; Jung, C.; Li, H.; Yu, M.; Flora, J.R.V.; Boateng, L.K.; Her, N.; Zoh, K.D.; Yoon, Y. Adsorption characteristics of diclofenac and sulfamethoxazole to graphene oxide in aqueous solution. *Chemosphere* **2015**, *136*, 20–26. [[CrossRef](#)] [[PubMed](#)]
17. Wang, J.; Zhang, P.; Yang, L.; Huang, T. Adsorption characteristics of construction waste for heavy metals from urban stormwater runoff. *Chin. J. Chem. Eng.* **2015**, *23*, 1542–1550. [[CrossRef](#)]
18. Dehou, S.C.; Wartel, M.; Recourt, P.; Revel, B.; Mabingui, J.; Montiel, A.; Boughriet, A. Physicochemical, crystalline and morphological characteristics of bricks used for ground waters purification in Bangui region (Central African Republic). *Appl. Clay Sci.* **2012**, *59*, 69–75. [[CrossRef](#)]
19. Meng, Q.; Wang, Z.; Chai, X.; Weng, Z.; Ding, R.; Dong, L. Fabrication of hematite (α -Fe₂O₃) nanoparticles using electrochemical deposition. *Appl. Surf. Sci.* **2016**, *368*, 303–308. [[CrossRef](#)]
20. Salem Attia, T.M.; Hu, X.L.; Yin, D.Q. Synthesized magnetic nanoparticles coated zeolite for the adsorption of pharmaceutical compounds from aqueous solution using batch and column studies. *Chemosphere* **2013**, *93*, 2076–2085. [[CrossRef](#)] [[PubMed](#)]
21. Schwertmann, U.; Cornell, R.M. *Iron Oxides in the Laboratory Preparation and Characterization*; Wiley: Weinheim, Germany, 2000.
22. Ghanizadeh, G.; Ehrampoush, M.H.; Ghaneian, M.T. Application of iron impregnated activated carbon for removal of arsenic from water. *Iran. J. Environ. Health Sci. Eng.* **2010**, *7*, 145–156.
23. Li, W.; Wang, L.; Liu, F.; Liang, X.; Feng, X.; Tan, W.; Zheng, L.; Yin, H. Effects of Al³⁺ doping on the structure and properties of goethite and its adsorption behavior towards phosphate. *J. Environ. Sci.* **2016**, *45*, 18–27. [[CrossRef](#)] [[PubMed](#)]
24. Ho, Y.S. Review of second-order models for adsorption systems. *J. Hazard. Mater.* **2006**, *136*, 681–689. [[CrossRef](#)] [[PubMed](#)]

25. Sun, K.; Shi, Y.; Wang, X.; Li, Z. Sorption and retention of diclofenac on zeolite in the presence of cationic surfactant. *J. Hazard. Mater.* **2017**, *323 Pt A*, 584–592. [[CrossRef](#)]
26. Muthukumaran, C.; Sivakumar, V.M.; Thirumarimurugan, M. Adsorption isotherms and kinetic studies of crystal violet dye removal from aqueous solution using surfactant modified magnetic nanoadsorbent. *J. Taiwan Inst. Chem. Eng.* **2016**, *63*, 354–362. [[CrossRef](#)]
27. Huang, B.; Xiong, D.; Zhao, T.; He, H.; Pan, X. Adsorptive removal of PPCPs by biomorphic HAP templated from cotton. *Water Sci. Technol.* **2016**, *74*, 276–286. [[CrossRef](#)] [[PubMed](#)]
28. Thanhmingliana; Tiwari, D. Efficient use of hybrid materials in the remediation of aquatic environment contaminated with micro-pollutant diclofenac sodium. *Chem. Eng. J.* **2015**, *263*, 364–373. [[CrossRef](#)]
29. Shu, J.; Wang, Z.; Huang, Y.; Huang, N.; Ren, C.; Zhang, W. Adsorption removal of Congo red from aqueous solution by polyhedral Cu₂O nanoparticles: Kinetics, isotherms, thermodynamics and mechanism analysis. *J. Alloys Compd.* **2015**, *633*, 338–346. [[CrossRef](#)]



© 2018 by the authors. Licensee MDPI, Basel, Switzerland. This article is an open access article distributed under the terms and conditions of the Creative Commons Attribution (CC BY) license (<http://creativecommons.org/licenses/by/4.0/>).